Spectral Analysis of the Airy Pulsed Beam

Yan Kaganovsky, and Ehud Heyman

School of Electrical Engineering, Tel Aviv University, Tel-Aviv, 69978, Israel

Abstract

The Airy beam (AiB) has attracted a lot of attention recently because of its intriguing features such as propagation along *curved* trajectories in free-space and the weak diffraction. Here we derive a class of ultra wide band (UWB) Airy pulsed beams (AiPB) which are the extension of the AiB into the time domain. We introduce a frequency scaling that renders the ray skeleton of the field frequency independent, thus insuring that the resulting AiPB is non-dispersive and preserves the intriguing features of the time-harmonic AiB. An exact closed form solution for the AiPB is derived using the spectral theory of transients (STT).

1. Introduction

Recently, a class of Airy beam (AiB) solutions of the paraxial wave equation has been introduced [1, 2]. These solutions have attracted a lot of attention because of their intriguing features, the most distinctive ones are the propagation along *curved* trajectories in free-space and the weak diffraction [2]. In a previous paper [3], we provided a cogent physical description to the AiB and its intriguing properties. We found that the AiB is a caustic of rays that radiate from the tail of the aperture distribution and then focus on the caustic which delineates, in fact, the beam's trajectory (Fig. 1). In this paper, we derive a class of ultra wide band (UWB) Airy pulsed beams (AiPB) which are the extension of the AiB into the time domain. Using the ray interpretation in [3] we introduce a frequency scaling of the initial aperture field that renders the ray skeleton of the field frequency independent (see Sec. 2), thus ensuring that all the frequency components propagate along the same curved trajectory, and that the resulting Airy pulsed beam (AiPB), derived in Sec. 3, does not disperse.

2. Non Dispersive Airy Beams: Frequency Domain (FD) Representation

The finite-energy Airy beam field $\hat{U}(x,z)$ in the half-space $z>0$ is generated by the aperture field distribution in at $z=0$

$$\hat{U}_0(x';\omega)=\exp(\alpha k x')\mathrm{Ai}(\beta^{-1/3}k^{2/3}x'), \tag{1}$$

where x' denotes points in the aperture, β and α are frequency-independent parameters, Ai is the Airy function, and $k=\omega/c$, with c the wave-speed assumed constant. $\exp(\alpha k x')$ is added in order to render the energy of this distribution finite. Here and henceforth, over hats denote FD constituents with time-dependence $\exp(-i\omega t)$. Since our goal here is to obtain an ultra wide band (UWB) solution, we chose the scaling factors in (1) to yield a *frequency independent* ray skeleton, in which the rays emerge from the aperture at local angles $\theta_0(x')=\sin^{-1}(-x'/\beta)^{1/2}$ (Fig. 1 and [3]). This scaling, unlike previous suggestions [4], ensures that all frequency components of the field are AiB's that propagate along the same trajectory, so that the resulting AiPB does not disperse and preserves the intriguing features of the time-harmonic AiB.

3. Time Domain Solutions: Airy Pulsed Beams

We start with the spectral (plane-wave) representation for the FD field,

$$\hat{U}(\mathbf{r};\omega)=\frac{\omega^{1/3}}{2\pi}\int_{\mathcal{C}}Ae^{i\omega\tau(\xi)}d\xi,\qquad A=(\beta/c)^{1/3},\qquad \tau(\xi;\mathbf{r})=\beta(\xi+i\alpha)^3/3c+\xi x/c+\zeta z/c, \tag{2}$$

where the spectral variable $\xi=\sin^{-1}\theta$ has a *frequency-independent* geometrical interpretation with θ being the plane-wave angle. Eq. (2) is obtained by taking the spectral representation of the aperture field at $z=0$ of (1), and multiplying by the spectral propagator $e^{ik\zeta z}$, where $\zeta=\sqrt{1-\xi^2}$, with $\mathrm{Im}\,\zeta\geq 0$ for $\omega>0$. The integration contour $\mathcal{C}$ extends along the real ξ axis from $-\infty$ to ∞, passing above and below the branch points $\xi=\mp 1$, respectively. In order to transform (2) into the TD, we shall use the analytic signal representation obtained via the one-sided Fourier transform,

978-1-4244-6051-9/11/$26.00 ©2011 IEEE

$$\overset{+}{u}(\mathbf{r},t)=\frac{1}{\pi}\int_0^\infty d\omega e^{-i\omega t}\,\hat{f}(\omega)\hat{U}(\mathbf{r};\omega),\quad \mathrm{Im}\,t\le 0, \tag{3}$$

where $\hat{f}(\omega)$ is an arbitrary temporal spectrum. Since the integral converges for real t, it also converges for all $t\in\mathbb{C}^-$, the lower half of the complex plane, thus defining an analytic function there. Here and henceforth we use an over + symbol to denote analytic signals. For simplicity we use in (3) $\hat{f}(\omega)=\omega^{-1/3}(-i\omega)^m\exp(-\omega T)$ where $m=0,1,2...$, the parameter $T>0$ is proportional to the pulse length and the factor $(-i\omega)^m$ suppresses the low frequencies (in the numerical example below we use $m=2$). We then substitute (2) into (3), use the condition $\mathrm{Im}\,t\le 0$ in order to switch the order of the ξ and ω integrations, and evaluate the ω integration in closed form to obtain

$$\overset{+}{u}(\mathbf{r},t)=\partial_t^m\frac{-i}{2\pi^2}\int_{\mathcal{C}}\frac{A}{t-\tau(\xi)-iT}d\xi. \tag{4}$$

Eq. (4) is denoted as the *STT integral* which represents the field as a spectrum of transient plane-waves. The integral has time-dependent poles $\xi(t)$ in the complex ξ plane, defined by $\tau[\xi(t)]=t-iT$. Concentrating on the relevant time window near the pulse arrival, the solutions $\xi(t)$ are depicted in Fig. 3. Actually there are additional poles here but their contributions can be neglected in the pertinent time window (see [6] for a full spectral analysis). By closing the integration contour at infinity about the lower or the upper half of the complex ξ-plane, the field is expressed as contributions from the poles $\xi(t)$ lying in the respective half plane, plus a contribution from the branch-cuts of ζ which can be neglected since they correspond to the evanescent spectrum (again see [6] for a full analysis). The analytic field of the AiPB is thus given by

$$\overset{+}{u}(\mathbf{r},t)=\sum_{p=1,2}\partial_t^m\frac{A}{\pi\tau'[\xi^{(p)}(t)]}=-\partial_t^m\frac{A}{\pi\tau'[\xi^{(3)}(t)]}, \tag{5}$$

where $\tau'=\partial_\xi\tau$, and the first and second expressions have been obtained by a lower or upper half plane closure, expressing the field as contributions from the poles $\xi^{(1,2)}(t)$ or $\xi^{(3)}(t)$ in the respective plane (see Fig. 3). Finally, the physical field for real t is obtained by taking the real part for $\mathrm{Im}\,t\uparrow 0$.

Figs. 3(b,d,f) show the fields calculated by using (5) with the second alternative. On the lit side of the caustic (Fig. 3(b)) there are two separate peaks at $t_{1,2}$, which are obtained when the pole $\xi^{(3)}(t)$ passes near the stationary points $\xi_{1,2}$ in Fig. 3(a) where τ' vanishes so that $\tau'[\xi^{(p)}(t)]$ in the denominator of (5) is small. On the caustic (Figs. 3(d)), these two peaks coalesce to a stronger peak, obtained when the pole passes near the second order stationary point ξ_c in Fig. 3(c). Finally, on the shadow side of the caustic (Figs. 3(f)), the pulse evanesces, as follows also from the fact that the pole passes far away from the real ξ axis. Fig. 2. shows a snapshot of the field in the xz plane for a fixed t. One observes that on the lit side of the caustic the field consists of two wavefronts which coalesce on the caustic, and on the shadow side the field decays.

Acknowledgments. This work is supported in part by the Israeli Science Foundation, under Grant No. 674/07.

References

[1] G. A. Siviloglou, J. Brokly, A. Dogariu, and D. N. Christodoulides, "Observation of Accelerating Airy Beams," *Phys. Rev. Lett.* **99** (2007).

[2] G. A. Siviloglou, and D. N. Christodoulides, "Accelerating Finite Energy Airy Beams," *Opt. Lett.* **32**, 979–981 (2007).

[3] Y. Kaganovsky, and E. Heyman, "Wave Analysis of Airy Beams," *Opt. Express* **18**, 8440–8452, (2010).

[4] P. Saari, "Laterally Accelerating Airy Pulses," *Opt. Express* **16**, 10303–10308 (2008).

[5] E. Heyman and L.B. Felsen, "Weakly Dispersive Spectral Theory of Transients (STT), Part I/II/III," *IEEE Trans. Antennas Propagat.* **35**, 80–86/574–580/1258–1266 (1987).

[6] Y. Kaganovsky and E. Heyman, "Airy Pulsed Beams," *submitted to J. Opt. Soc. Am. A.*

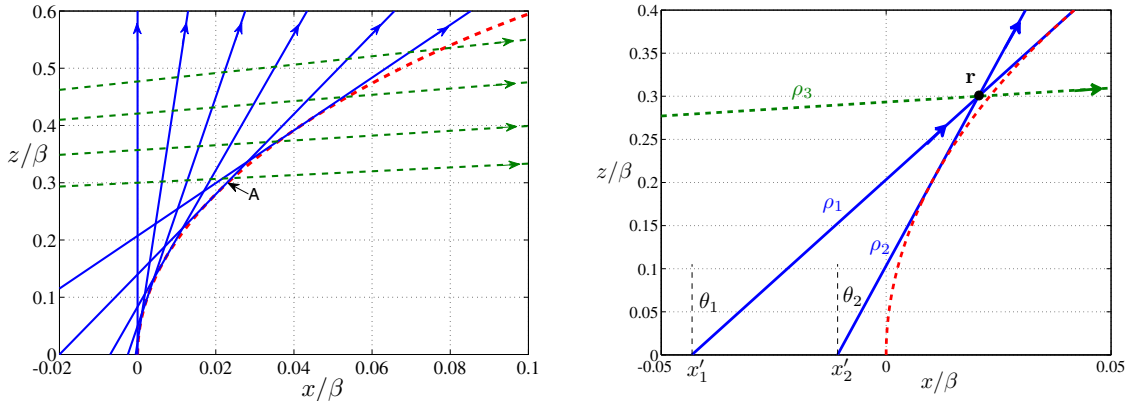

(a) Ray skeleton (b) Rays for observation point **r**

Figure 1: (a) Ray representation of the AiB. The solid (blue) rays radiate from the aperture at $z = 0$ and focus onto a caustic (thick red dashed line) which delineates the beam's propagation trajectory. The dashed (green) rays radiate from distant points where the aperture field is weak and arrive to the region of the caustic at late times. These rays are therefore neglected in the present analysis (for a complete analysis see [6]). Accordingly, the regions on the left and right sides of the caustic are referred to as the "lit" and "shadow" sides, respectively. For the UWB AiPB, the same ray skeleton is used for all frequencies. Also showing point A where the field will be calculated in the sequel. (b) Ray contributions for a point **r** on the lit side of the caustic near point A. Rays 1,2 leave the aperture at $x_1' = -0.043\beta$, $x_2' = -0.011\beta$, with exit angles $\theta_{1,2}$, and arrive at **r** at $t = t_{1,2}$, respectively. Ray 1 touches the caustic after reaching **r**, while ray 2 touches the caustic before **r**. Ray 3 originates at a distant point and will not be considered in the present analysis, as mentioned above.

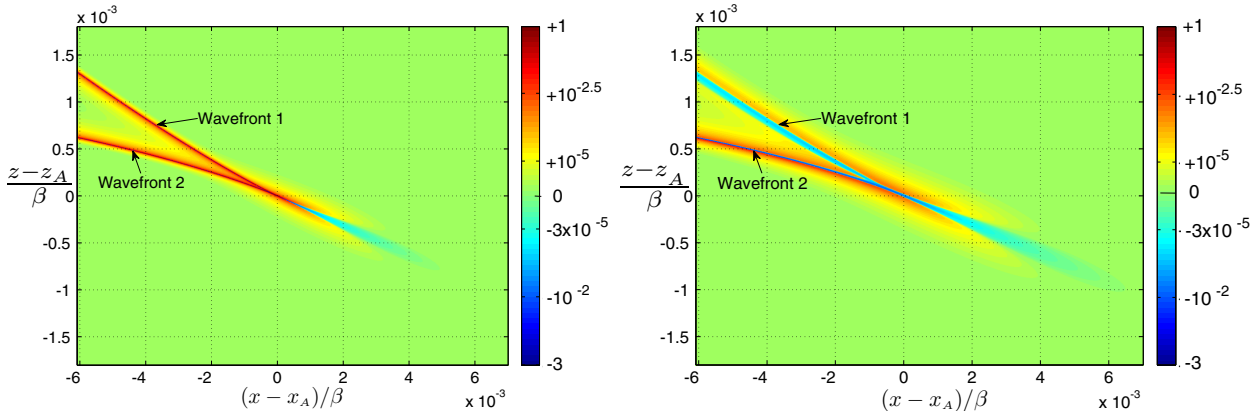

(a) $\alpha = 10^{-5}$ (b) $\alpha = 10^{-3}$

Figure 2: Snapshots of the field near point A on the caustic, defined in Fig 1. The snapshots are taken at $t = t_{\rm A}$ = the time of arrival at A. The axes are centered around point A and normalized with respect to β. The signal parameters are $m = 2$, $T = 10^{-6}\beta/c$ with $\alpha = 10^{-5}$ in (a) and $\alpha = 10^{-3}$ in (b) (see (2) and (4)). The logarithmic color scale retains the sign of the waveform (see color bar). The fields are normalized with respect to the maximal value. One readily observes that the field consists of two wavefronts which coalesce on the caustic. Wavefronts 1,2 are formed by rays of species 1,2, respectively, which are depicted in Fig. 1(b). Increasing α in (b) affects essentially wavefront 1 since the rays of species 1 originate from the aperture at points that are located further away from the center and are therefore strongly affected by the exponential decay (see (1)). Increasing α also increases the pulse width, as seen by comparing (b) to (a).

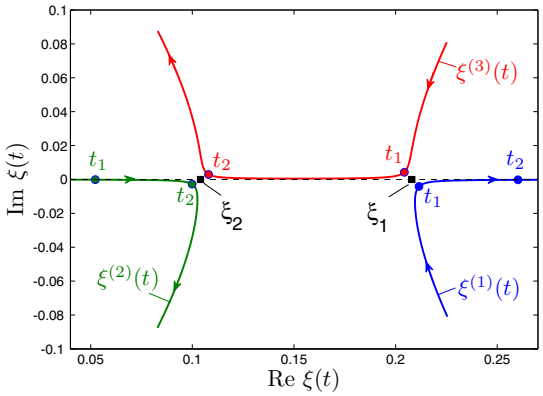

(a) Poles for the lit side of the caustic

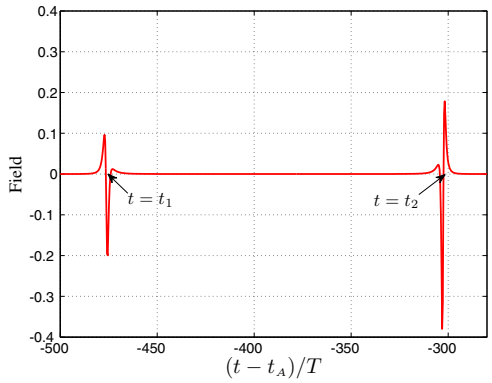

(b) Field on the lit side of the caustic.

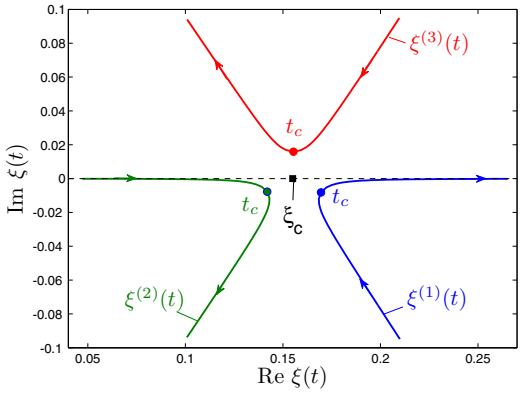

(c) Poles for the caustic

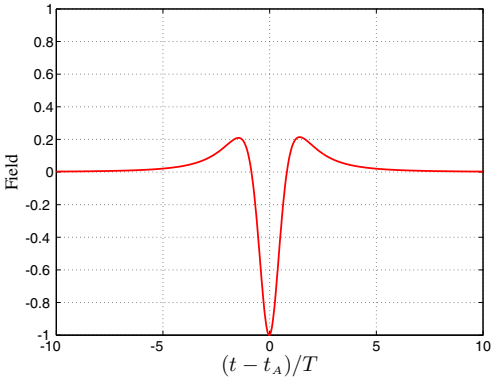

(d) Field on the caustic.

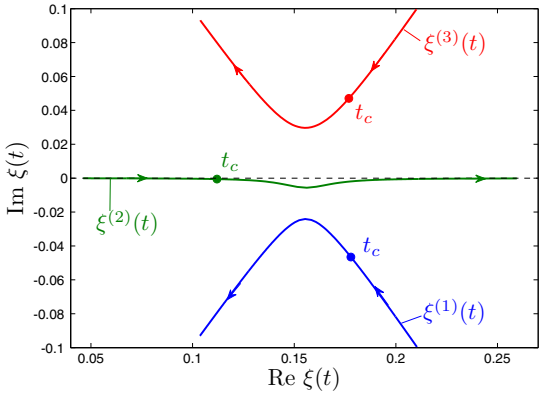

(e) Poles for the shadow side of the caustic.

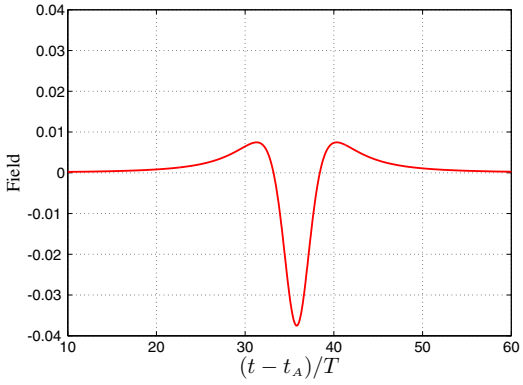

(f) Field on the shadow side of the caustic.

Figure 3: (a,c,e) and (b,d,f): trajectories of the poles of (4) and the corresponding field waveforms, respectively, for observation points near point A on the caustic. (a,b) Observation point on the lit side of the caustic (see Fig. 1(b)) ; (c,d) on the caustic; (e,f) on the shadow side of the caustic. These points are displaced horizontally from A by Δ_x where $\Delta_x = -2.5\,10^{-3}\beta$, 0, and $2.3\,10^{-4}\beta$, respectively. Square tags: stationary points $\xi_1 = 0.208$ and $\xi_2 = 0.104$ corresponding to rays 1,2 of Fig. 1(b) with exit angles $\theta_{1,2} = \sin^{-1}(\xi_{1,2})$ and arrival times $t = t_{1,2}$. On the caustic, the two stationary points coalesce $\xi_1 = \xi_2 = \xi_c$ and both rays arrive at $t = t_c$. In (b,d,f) the field has been calculated by using (5) with the second alternative. The time axis is centered around $t_{\rm A}$ (the time of arrival to point A) and normalized with respect to T. The signal parameters are $m = 2$, $T = 10^{-6}\beta/c$ and $\alpha = 10^{-5}$ (see (2) and (4)). Notice the differences in the scales of the figures. The field is normalized such that $\max|\overset{+}{u}| = 1$. Note that away from the caustic on the lit side, the field is described by the arrivals of rays 1,2, as seen in (b).